Available online at www.sciencedirect.com
ScienceDirect
Journal of Sound and Vibration 311 (2008) 537–553
JOURNAL OF SOUND AND VIBRATION
www.elsevier.com/locate/jsvi

Recovery of vibration signal based on a super-exponential algorithm

Yujun Li, Peter W. Tse*, Xiaojuan Wang

Smart Engineering Asset Management Laboratory (SEAM), Department of Manufacturing Engineering & Engineering Management, City University of Hong Kong, Tat Chee Avenue, Kowloon, Hong Kong, China

Received 18 September 2007; accepted 23 September 2007
Available online 5 November 2007

Abstract

Vibration-based analysis is an important technique in machine fault diagnosis. In complex machines, the vibration generated by a component is easily affected by the vibration of other components or is corrupted by noise from other sources. Hence, the fault-related vibration must be recovered from among those sources for accurate diagnosis. In this paper, a super-exponential algorithm (SEA) based on the single-input single-output (SISO) convolution mixing model is investigated to deconvolve the vibration signal of interest. Based on simulated vibration signals generated by a test bench in a laboratory and real signals generated by industrial machines, the characteristics of the SEA with skewness and kurtosis schemes are studied extensively for the recovery of signals with different statistical distributions. It is shown that the SEA with the skewness scheme is more suitable for the isolation of a vibration signal with an asymmetric distribution, whereas the SEA with the kurtosis scheme is more efficient for detecting a vibration with abrupt changes in its distribution. Furthermore, the effect of the equalizer length on the characteristics of the equalized signal is discussed. A performance curve that presents the equalization performance is defined, and a method that uses this curve to select the optimal equalizer length for successfully recovering the defect signal from the mixed signal is then proposed. The study presented in this paper thus shows that the SEA is a promising method for the recovery of vibrations in machine fault diagnosis.

1. Introduction

Vibration-based analysis for fault diagnosis has received a great deal of attention in recent years because the results are directly related to the rotational characteristics of mechanical components. It has also been increasingly used in industry to achieve a high level of reliability with fewer breakdowns due to the early detection of defects in machines. However, the vibration signal generated in a machine is easily contaminated by vibrations from other sources, or corrupted by noises from the structural vibration of the machine. In such situations, it is difficult to extract the vibration signal of interest for accurate fault diagnosis. For example, the detection of a localized defect in early stages is still a problem because the measured signal is affected by the harmonics from rotating components of the machine and the impulses generated by defects. Hence, it is

*Corresponding author. Tel.: +852 27888431; fax: +852 27888423.
E-mail address: MEPTSE@cityu.edu.hk (P.W. Tse).

0022-460X/$ - see front matter © 2007 Elsevier Ltd. All rights reserved.
doi:10.1016/j.jsv.2007.09.036

essential to find an efficient method for machinery fault diagnosis that can recover the fault-related vibration from a mixed signal. Numerous approaches, such as higher-order statistics [1], the wavelet transform [2,3], and the Hilbert–Huang transform [4], have been developed to achieve this objective. However, the robustness and accuracy of these methods in extracting the fault features sharply decrease when the background noise is high or the signal of interest is distorted during transmission from the source position to the measurement point.

Recently, blind signal processing techniques have been successfully applied to engineering problems in various industrial fields for the recovery or extraction of signals. These techniques were initially used in communications to mitigate the multi-path fading and noise effects from transmission channels with a measured signal. The major advantage of this technique is that it does not require any prior knowledge of the source signals and transmission path. Linear principal components analysis (PCA) was probably the first blind technique to be used that was based on second-order data statistics [5]. An important extension of PCA is known as independent components analysis (ICA). Another promising method named blind equalization (BE) was introduced by Sato and has since become one of the key techniques used in the field of digital communications [6] to recover voice or picturephone signals after transmission over the frequency-division multiplexed transmission channel. Donoho presented an overview of the initial solutions of blind deconvolution (BD) [7], the fundamental idea of which was to derive from the received signal the equalizer characteristics based on high-order cumulants. This means that knowledge of the sources and input channels of the received signals is not required. Of these methods, BE has demonstrated solid achievements in communications and is a prospect for wider applications. However, the efficiency of BE for vibration recovery in the mechanical field has not been widely proved, with only a few studies published on relevant topics. Li et al. [8] reviewed the application of blind source separation (BSS) in machine fault diagnosis, and Alexander et al. [9] proposed the use of BSS to isolate a machine signature from distorted measurements. After an in-depth analysis, they concluded that the instantaneous mixing model may be valid in acoustic monitoring, and that a convolutive mixture model is appropriate for vibration monitoring. Gelle et al. [10] proposed two approaches to solving the BSS problem for rotating machine signals, and illustrated the potential of those approaches as a pre-processing step to improve diagnosis. Lee and Nandi [11] studied the application of two BD algorithms, the objective function method (OFM) and the eigenvector algorithm (EVA), to extract impulsive impacting signals. The algorithms performed well, and the study demonstrated that BE is a promising technique for the extraction of vibration signals from contaminated sources. In this paper, the application of the super-exponential algorithm (SEA) [12] to the recovery of mechanical vibration signals is investigated. Based on simulation and experimental analysis, the performance of the SEA with both skewness and kurtosis schemes for recovering vibration signals with different statistics is proposed and investigated. Furthermore, the effect of the equalizer length used in the SEA on the equalized signal is discussed, and a new method to obtain an optimal equalizer length is proposed.

The structure of the rest of this paper is as follows. In Section 2, the basic theory of BE and the SEA are reviewed. Section 3 introduces the distribution characteristics of the third-order (skewness) and fourth-order (kurtosis) statistics, and the principle of selection of the kth-order statistic scheme in the SEA for different signals is proposed. In Section 4, the effect of the equalizer length on the result of the SEA is analyzed, and a principle for selecting an equalizer length to achieve the optimal equalized result in practical applications is proposed.

2. Brief review of blind equalization and the super-exponential algorithm

2.1. Brief review of blind equalization

A schematic model of single-input single-output (SISO) BE is shown in Fig. 1. The measured signal $x[n]$ contains two parts. One part is $x_s[n]$, which is the output process of an unknown linear time-invariant (LTI) system $h[n]$, where the original signal $s[n]$ is the system input. Note that it is not possible to observe $s[n]$ directly. The other part is $w[n]$, which is the additive noise signal that can be described by the following equation:

$$x[n] = x_s[n] + w[n], \tag{1}$$

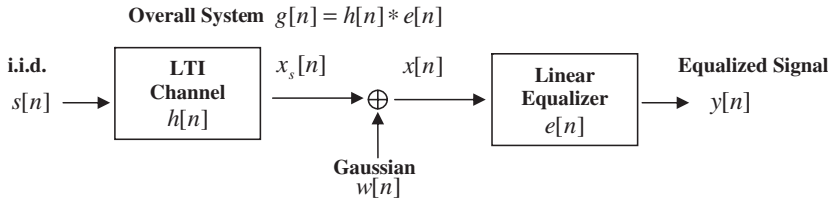

Fig. 1. Schematic model of SISO blind equalization.

where

$$x_s[n] = h[n]s[n] = \sum_{i=0}^{M} h[i]s[n-i], \tag{2}$$

where M is the length of the unknown impulse response system $h[n]$ (an infinite length). The original signal $s[n]$ is uncorrelated with the noise $w[n]$.

The output of equalizer $y[n] = e[n] * x[n]$ is the convolution result of $x[n]$ and the linear equalizer $e[n]$. The aim of BE is to make $y[n]$ approximately equal to input $s[n]$ through the optimization of the equalizer by adjusting its parameters. Here, an overall system response is defined as $g[n] = h[n] * e[n]$, that is, the unknown channel convolves with the equalizer. According to the definition of BE, the following equation is validated:

$$g[n] = \mathrm{e}^{j\phi}\delta_{n-k} = \begin{cases} \mathrm{e}^{j\phi}, & n = k, \\ 0, & n \neq k, \end{cases} \tag{3}$$

where k stands for the time delay and ϕ stands for the phase shift. This is the main idea of BE based on the SISO mixing model.

According to this description, BE does not require prior knowledge of the source signal. However, the following assumptions (conditions) must hold for successful extraction of the source signal.

S-H1: The LTI system $h[n]$ is a stable possibly non-minimum phase LTI filter for which the inverse $h[n]^{-1}$ exists.

S-H2: The source signal $s[n]$ is a zero-mean independently and identically distributed (i.i.d.) non-Gaussian random process with a variance $\sigma_s^2 = E\{|s[n]|^2\}$ and a $(p+q)$th-order cumulant $\gamma_{p,q} = \mathrm{cum}(s[n] : p, s^*[n] : q) \neq 0$, where the superscript '*' denotes complex conjugation, p and q are non-negative integers, $p + q \geqslant 3$, $E\{|s[n]|^2\}$ denotes the expectation of process $s[n]$ and $\mathrm{cum}(s[n] : p, s^*[n] : q)$ denotes the $(p+q)$th-order cumulant of process $s[n]$.

S-H3: The noise $w[n]$ is a zero-mean Gaussian random process and is statistically independent of $s[n]$.

Alexander et al. [9] highlighted that dispersion and reverberation can severely distort waveforms which are indicative of faults. These distortions may be reflected by the convolution of the mixing model, and thus in mechanical vibration analysis the LTI system refers to the transmission paths of the inspected signal from different sources to the measured point. When a machine is operating in stable conditions, the transmission path fulfils assumption **S-H1**, and the source vibration signal is i.i.d. with a non-Gaussian process, which satisfies assumption **S-H2**. Consequently, the assumptions of the mixing model can be theoretically validated through the application of BE algorithms to mechanical vibration analysis.

2.2. Brief review of SEA

Shalvi and Weinstein [12] found the optimum $e[n]$ by maximizing $J_{p,q}(e)$, or the inverse filter criteria, which is the objective function of the linear equalizer $e[n]$ with only two cumulants:

$$J_{p,q}(e) = \frac{|\mathrm{cum}\{y[n] : p, y^*[n] : q\}|}{[\mathrm{cum}\{y[n], y^*[n]\}]^{(p+q)/2}}, \tag{4}$$

where p and q are non-negative integers ($p+q \geqslant 3$), the superscript '*' denotes complex conjugation, cum$\{y[n]: p, y^*[n]: q\}$ denotes the $(p+q)$th-order cumulant of process $y[n]$, and $y[n]$ denotes the equalized signal.

The equalizer $e[n]$ is assumed to be a finite impulse response (FIR) filter over the interval $L_1 \leqslant L \leqslant L_2$ with a length $L = L_2 - L_1 + 1$, and it is defined as follows:

$$\mathbf{e} = [e[L_1], e[L_1+1], \ldots, e[L_2]]^{\mathrm{T}}. \tag{5}$$

At the ith iteration, the SEA updates the vector $\mathbf{e}$ through the following set of linear equations:

$$\begin{cases} \mathbf{e} = (\mathbf{R}_x)^{-1} \cdot \mathbf{d}_{yx}^{[i-1]}, \\ \mathbf{e}^{[i]} = \mathbf{e}/||\mathbf{e}||, \end{cases} \tag{6}$$

where $||\mathbf{e}||$ denotes the norm of vector $\mathbf{e}$, $(\mathbf{R}_x)^{-1}$ denotes the inverse of $\mathbf{R}_x$, and $\mathbf{R}_x$ is the $L \times L$ correlation matrix of $x[n]$

$$R_{i,j} = \mathrm{cum}(x[n-i], x[n-j]) \tag{7}$$

and $\mathbf{d}_{yx}^{[i-1]} = [d_0, d_1, \ldots, d_{-L+1}]^{\mathrm{T}}$ is the $L \times 1$ vector. Its elements are joint cumulants of the equalized signal $y[n]$ and the observed signal $x[n]$:

$$d_i = \mathrm{cum}(y[n]: p, y^*[n]: q-1, x^*[n-i]). \tag{8}$$

When the SEA converges, the linear equalizer $e[n]$ from $\mathbf{e}^{[i]}$ and the equalized signal $y[n]$ can be obtained. The computation of the SEA is efficient because of its fast convergence at a super-exponential rate.

Shalvi and Weinstein [12] introduced two types of filter criteria, and employed two values of $p+q$ (3 or 4) in the objective function $J_{p,q}(e)$. When $p=1$, $q=2$, $p+q=3$, which corresponds to the third-order statistic scheme, $J_{p,q}(e)$ denotes the skewness of the equalized signal $y[n]$, and when $p=2$, $q=2$, $p+q=4$, which corresponds to the fouth-order statistic scheme, and $J_{p,q}(e)$ denotes the kurtosis of $y[n]$.

The SEA has shown good performance in voice recognition, communications [13], and image processing [14] applications, and thus its application in the mechanical field is proposed in this paper. Potential problems with applying the SEA include its feasibility for extracting the vibration of interest from mixed sources, and parameter selection to improve the equalized performance. Investigation and discussion of these issues are presented in detail in the following sections.

3. Analysis of the SEA with kth-order statistic scheme

The SEA can use the skewness ($p+q=3$) or kurtosis ($p+q=4$) of the equalized signals as its objective function. However, the skewness and kurtosis schemes have very different levels of effectiveness for vibrations in different applications, and it has been found that they are closely related to the distribution of signals. In this section, the properties of skewness and kurtosis are discussed, and conclusions are drawn on how to choose the kth-order statistics as equalization criteria for signals with different distribution features.

3.1. Characteristics of skewness and kurtosis

Skewness and kurtosis are both measurements of process distribution and denote the non-Gaussian index of a process. For a Gaussian distribution process, skewness is zero and kurtosis is around 3. Hence, the effect of Gaussian noise can be decreased by the SEA with these two measurements, which consequently allows the signal features to be presented tangibly.

Skewness: Skewness is a measure of symmetry distribution and it characterizes the degree of asymmetry of a distribution around its mean. A distribution or a dataset is regarded to be symmetrical if it is equal at the top and bottom around the center point. Examples of distributions with different skewness values are shown in Fig. 2(a). Skewness is defined as follows:

$$\mathrm{Skewness}(y[1] \ldots y[N]) = \frac{1}{N} \sum_{i=1}^{N} \left[\frac{y[i] - \bar{y}}{\sigma} \right]^3, \tag{9}$$

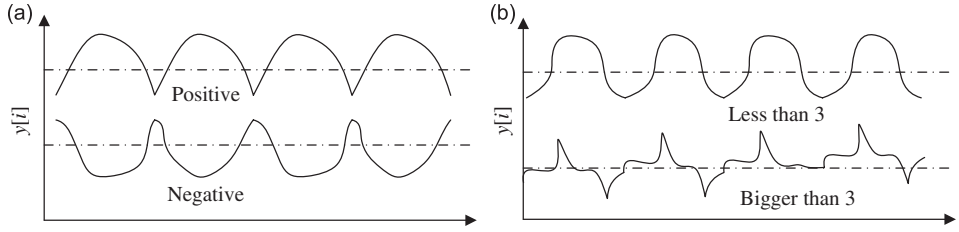

Fig. 2. Skewness and kurtosis of different distribution series: (a) skewness and (b) kurtosis.

where $\sigma = (1/(N-1))\sum_{i=1}^{N}(y[i]-\bar{y})^2$ is the distribution's standard deviation and $\bar{y} = (1/N)\sum_{i=1}^{N} y[i]$ is the mean value of $y[i]$. Any symmetrical distribution should have a near-zero skewness. For a temporal vibration signal, the center point denotes the mean value, and thus a negative skewness value indicates that the signal is skewed at the bottom (the negative part) and a positive skewness value indicates that the signal is skewed at the top (the positive part).

Kurtosis: Kurtosis shows the heaviness of the tails in the distribution of a sequence. Outliers or abrupt changes in the sequence produce a large kurtosis. The kurtosis of a standard distribution is 3. A kurtosis value bigger than 3 indicates a "peaked" distribution, and a value of less than 3 indicates a "flat" distribution, which is shown in Fig. 2(b). Kurtosis is defined as follows:

$$\text{Kurtosis}(y[1]\ldots y[N]) = \frac{1}{N}\sum_{i=1}^{N}\left[\frac{y[i]-\bar{y}}{\sigma}\right]^4, \tag{10}$$

where $\sigma = (1/(N-1))\sum_{i=1}^{N}(y[i]-\bar{y})^2$ is the standard deviation of the distribution and $\bar{y} = (1/N)\sum_{i=1}^{N} y[i]$ is the mean value of$y[i]$.

When the non-Gaussianity of a signal is larger, the tails of the sequence become heavier and its symmetry is destroyed. This results in a large kurtosis value, which implies that kurtosis can be used to establish an effective statistical test for the identification of abrupt changes in signals, such as those that occur in the vibration signals of defective bearings.

It is clearly shown that skewness describes the degree of asymmetry of a signal and kurtosis represents the abrupt changes in a signal. Hence, with different kth-order statistic schemes, the SEA uses different distribution indices as the objective function, and thus has different levels of ability to recover signals with different distribution properties. For example, for a non-Gaussian signal with near-zero skewness, which is similar to the noise, the SEA with the skewness scheme may produce an undesired equalized signal. It may also be difficult to achieve convergence because of the difficulties in differentiating the skew characteristics of the source signal from those of background noise. Hence, it is necessary to intensively research the applications of the SEA with various kth-order statistic schemes to accurately recover the signals that are related to machine defects.

3.2. Verifying the effectiveness of SEA with skewness and kurtosis by using simulated data

This section reports the effectiveness of the SEA with skewness and with kurtosis by using simulated bearing data. The characteristics of the two methods are also presented in relation to the recovery of mixed vibration signals, and their scope of application is then identified. The SEA with kurtosis is shown to be more effective in detecting the bearing fault than the SEA with skewness.

3.2.1. The simulation model of bearing

The SEA equipped with the skewness/kurtosis scheme detects the source based on the skewness/kurtosis of the equalized signal. The vibrations generated from the different machines exhibit the various characteristics of distribution. Hence, the SEA with skewness/kurtosis has the distinct ability to recover the specific source signal from the different obtained signals. To demonstrate this point, a simulation model of a bearing is introduced into the analysis of SEA with skewness/kurtosis.

3.2.1.1. The general model of bearing. According to a number of well-established models [15], impact is produced when a bearing defect or imperfection strikes one of the rolling elements. As the bearing rotates, the impact periodically occurs at a given frequency depending on the nature of the fault, the rotation speed and the bearing geometry. In addition, this impact periodically excites a number of natural frequencies of the bearing structure. The response pattern of the whole bearing vibration is that the natural frequencies of the bearing structure are modulated by the given frequency.

A theoretical model of a bearing with defective rolling elements introduced in Ref. [15] is used in this paper. Assuming that series $x(t)$ is the original signal from the rolling element bearing with a single fault, it can be modulated as

$$x(t) = x_f(t) * x_q(t) * x_{bs}(t) + x_s(t) + n(t), \tag{11}$$

where $x_f(t) * x_q(t) * x_{bs}(t)$ denotes the convolution results of $x_f(t)$, $x_q(t)$ and $x_{bs}(t)$ in time domain, $x_f(t)$ is the basic impulse series, which is produced by the fault that repetitiously strikes another surface in the bearing, $x_q(t)$ is the modulation effect caused by the non-uniform load distribution of the bearings and the cyclic variation of the transmission path between the fault impact site and the transducer, $x_{bs}(t)$ is the bearing-induced vibration, $x_s(t)$ is the machinery-induced vibration, and $n(t)$ is a Gaussian white noise sequence with a variance of σ_n^2.

3.2.1.2. A simplified model of a bearing with a common outer-race fault. The simplified case of a bearing with an outer-race defect based on the above model is considered here. It is assumed that the periodical non-uniform load distribution $x_q(t)$ does not modulate the impulse series $x_f(t)$ from the outer-race fault of the bearing. The bearings are set to run under a light load without consideration of mechanical vibration. Thus, the theoretical model for this specific case is as follows:

$$x(t) = x_f(t) * x_{bs}(t) + n(t). \tag{12}$$

In this case, the simulated signal $x(t)$ contains the basic impulse series generated by the repetitious strike of the outer race with the rolling elements, and the induced noise.

3.2.1.3. A simplified model of bearing with the common outer-race fault and misalignment. To further verify the effectiveness of the SEA in detecting bearing fault, the model of a bearing with an outer-race fault and the bearing shaft with misalignment was built. When misalignment occurs, the amplitudes of the rotational speed of the bearing shaft's fundamental frequency and its harmonics will be increased significantly in its related frequency spectrum, especially at the second harmonic of the fundamental frequency. In such a case, the model of the bearing becomes

$$x(t) = x_f(t) * x_{bs}(t) + x_s(t) + n(t), \tag{13}$$

where $x_f(t)$, $x_{bs}(t)$, $x_s(t)$, and $n(t)$ have been described in Eq. (11). The time signals generated by using Eq. (13) contain three components. The first component is induced by the bearing's vibration as well as the vibration generated by its outer-race fault. The second component is created by the mechanical vibration, and the third component is noise.

3.2.2. Verifying the results of the SEA with skewness and kurtosis in the detection of simulated bearing faults
3.2.2.1. Results of the simulated bearing with outer-race fault. Based on Eq. (12), a simulated signal was generated. It is assumed that the ball passing frequency of the outer race is 73.6 Hz, the frequencies of the bearing-induced vibration (bearing excitation frequency zone) are centered at 2000 Hz, and the signal ($x_f(t) * x_{bs}(t)$) to noise ($n(t)$) ratio (SNR) is 1 dB. The temporal waveform of simulated signal is shown in Fig. 3(a)(i). Due to a high level of noise corruption, it is difficult to distinguish the impulse components from the temporal waveform. The spectrum shown in Fig. 3(a)(ii) indicates a number of distinct frequency components (bearing excitation frequency zone) in a frequency band presumably from 1800 to 2200 Hz.

To demonstrate the different ability of the SEA with skewness and kurtosis, the SEA with these two schemes, in which the equalizer lengths were set to 16, was applied to the simulated signal. The equalized

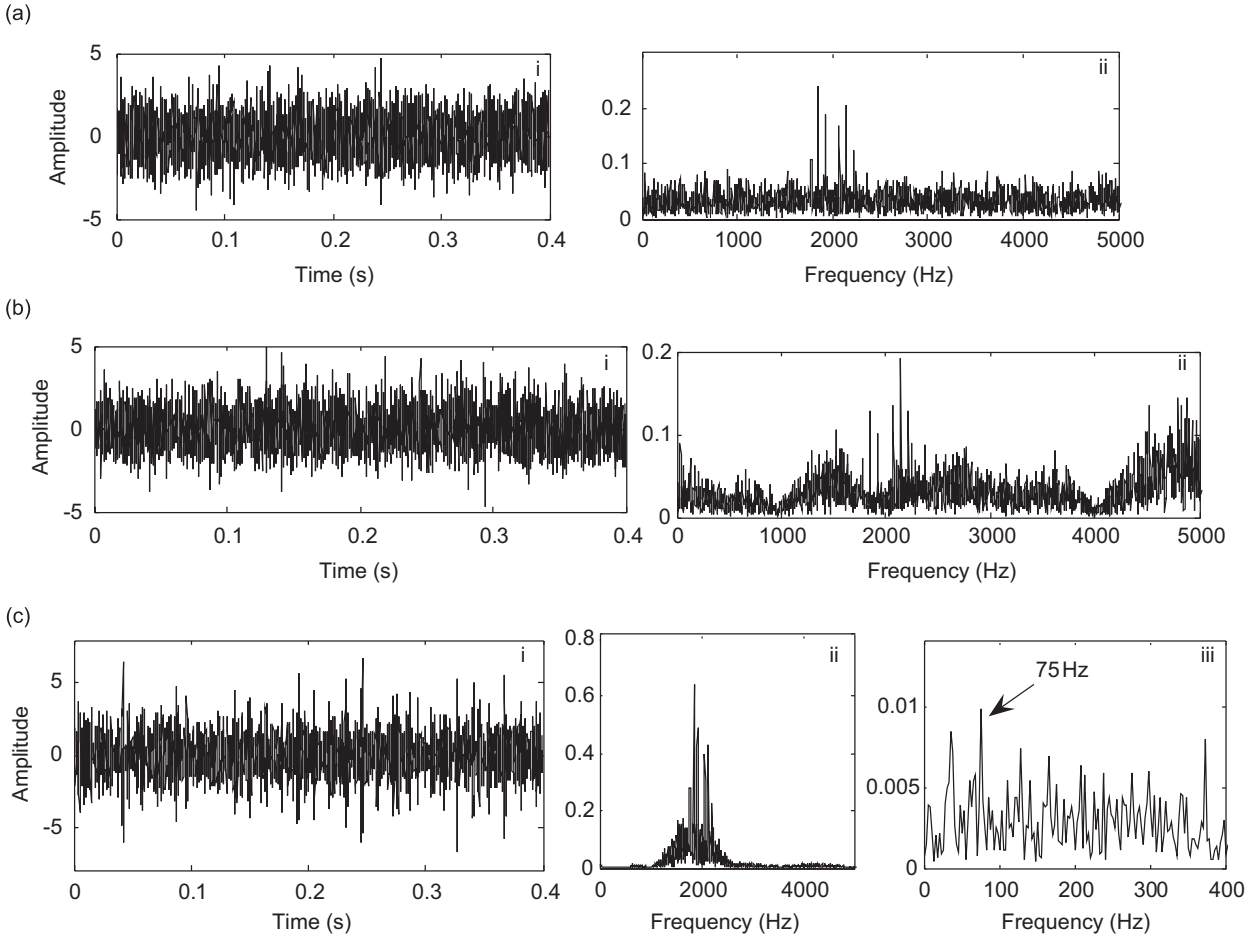

Fig. 3. Simulated bearing signal, equalized signals, and their spectra: (a) simulated signal and its spectrum; (b) equalized signal and its spectrum (skewness scheme); and (c) equalized signal and its spectra (kurtosis scheme).

signal and its spectrum obtained after using the SEA with the skewness scheme are shown in Figs. 3(b)(i) and (b)(ii), respectively. Fig. 3(c)(i) shows the temporal equalized signal obtained by using the SEA with the kurtosis scheme, and Figs. 3(c)(ii) and (c)(iii) show its spectrum and the low frequency part of the spectrum to highlight the relevant characteristic frequencies. In Fig. 3(b)(i), it is difficult to detect the impulse series induced by an outer-race defect on the bearing. In addition, unknown components appear in the high frequency band from 4000 to 6000 Hz shown in Fig. 3(b)(ii) compared with the spectrum in Fig. 3(a)(ii). Hence, the SEA with the skewness scheme cannot effectively detect the impulse series induced by the local defect, but introduces unknown components to the equalized signal, which obviously does not coincide with the aim of BE. The reason for this occurring is that the skewness of the simulated signal is close to zero (-0.0218) because of the symmetry of the bearing vibration in time distribution, which does not meet assumption **S-H2** of BE.

In contrast, when the kurtosis scheme is used, the equalized signal (Fig. 3(c)(i)) exhibits the impulse series, which is barely perceptible in the simulated signal of the bearing (Fig. 3a(i)), and the frequency spectrum plots of the equalized signal clearly show the bearing excitation frequency zone (a frequency band from 1800 to 2200 Hz) in Fig. 3(c)(ii) and the BPFO in Fig. 3(c)(iii) (75 Hz, close to the calculated BPFO of 73.6 Hz). Hence, the SEA with the kurtosis scheme has an excellent ability to detect the impulse series, whereas the SEA with the skewness scheme cannot be used to effectively recover the signal generated by the local defect from the mixed signals.

3.2.2.2. Results of the simulated bearing with outer-race fault and misalignment. Based on Eq. (13), a simulated signal was generated with the bearing outer-race fault described in the previous section and a misalignment of the bearing's shaft which was rotated at 15 Hz. Figs. 4(a)(i) and (a)(ii) show the equalized signal and its spectrum after the application of the SEA with the skewness scheme to the simulated signal. In Fig. 4(b)(ii), the fundamental frequency of the bearing's shaft and its harmonics located in the low frequency range remains, but the bearing-induced vibration frequencies are eliminated. Moreover, Fig. 4(b)(iii) clearly shows the increase of frequency components due to misalignment. According to vibration-based rotary machine fault diagnosis, misalignment brings a significant increase in the amplitude of the higher harmonics of the fundamental rotational frequency of the bearing's shaft. Fig. 4(b)(iii) clearly shows the harmonics of $2\times$ (30 Hz) up to $8\times$ (120 Hz). Hence, these results indicate that the SEA with the skewness scheme is effective in recovering the vibration signal related to misalignment or even imbalance, which has a high degree of asymmetric distribution (a large skewness value).

When the SEA with the kurtosis scheme is applied to the same simulated vibration signal, the equalized signal and its spectrum appear as in Figs. 4(c)(i) and (c)(ii), respectively. Fig. 4(c)(ii) shows that the

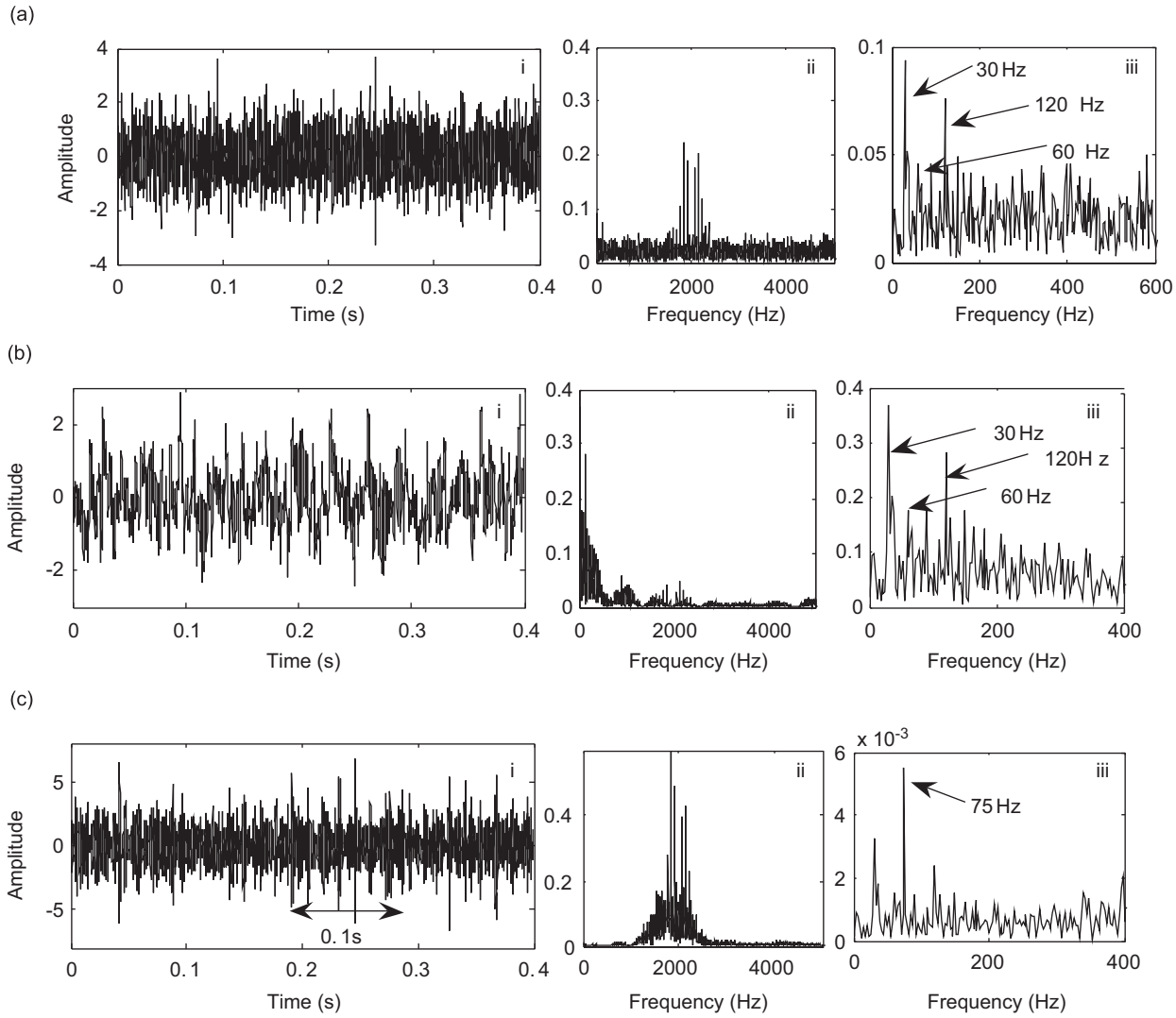

Fig. 4. Simulated signal (misalignment and outer-race defect), equalized signals, and their spectra: (a) simulated signal and its spectrum; (b) equalized signal and its spectrum (skewness scheme); and (c) equalized signal and its spectrum (Kurtosis scheme).

bearing-induced vibration frequency band from 1800 to 2200 Hz exists, and Fig. 4(c)(iii) highlights the BPFO frequency (75 Hz) and its harmonics. This result is confirmed in Fig. 4(c)(i), in which there are 7 impulses in 0.1 s from time 0.15 to 0.25, and the corresponding frequency is close to the calculated BPFO of 73.6 Hz. This equalized signal denotes the vibration generated by the bearing with an outer-race defect. Hence, the SEA with the kurtosis scheme has an extraordinary ability to extract vibration with abrupt changes, such as during bearing-defect-induced vibration.

3.3. *Verifying the effectiveness of the SEA with skewness and kurtosis using experimental data*

To confirm the conclusions in Section 3.2, experiments were conducted on a simulation test bench. The bench was used as a machinery fault simulator to generate the required vibration signals.

The simulation test bench is shown in Fig. 5. Its main components are a motor, two flywheels (III), and two bearings (I and II) that were used for mounting the shaft. Bearing (I) is a faulty component with a defect in the outer race, whereas bearing (II) is mechanically healthy. The shaft of the motor was connected to the shaft of the flywheels with a coupler, and no bolts were used on the flywheels. A small misalignment was introduced in the shaft between the motor and one of the flywheels. The shaft was rotated at a speed of 3000 rev/min, corresponding to the fundamental frequency of 50 Hz. Four accelerometers were installed in different positions to collect the required signals. The first sensor was located at the driving end of the motor (sensor 1). The second and fourth sensors were installed in the middle of the bearing house after the coupler of the shaft in the vertical and horizontal directions (sensors 2 and 4). The third sensor was mounted on the bearing house (II) at the end of the drive shaft (sensor 3). The vibrations from all sensors were captured at a sampling frequency of 10 kHz under the aforementioned configurations, and were then filtered by a low-pass filter with a cutoff frequency of 8 kHz for further processing.

Sensors 2 and 4 were located near the bearing (I) and the coupler, respectively, and the collected signals thus mainly revealed the vibrations generated by the bearing (I) and the misaligned shaft. The structural characteristic frequency of bearings generally occupies a high frequency range in the spectrum of their vibration, whereas the misalignment of a shaft mostly generates a vibration that is related to the frequency of the rotating speed (often twice the fundamental frequency), and is usually located in the low frequency range. Fig. 6(a) shows the spectrum of the observed signal of sensor 2. The low frequency components reflect the misalignment characteristics of the shaft and the resonance of the fundamental frequency (50 Hz). The components from 1500 to 4500 Hz are related to the characteristic frequencies of the bearing, which do not change with the rotating speed of the shaft. The SEA with the skewness and kurtosis schemes was applied to the signal captured from sensor 2. The length of the equalizers used in the SEA was set to 16. Fig. 6(b) indicates the spectrum of the equalized signal as given by the SEA with the skewness scheme, and Fig. 6(c) indicates the spectrum of the equalized signal as given by the SEA with the kurtosis scheme. A comparison of Fig. 6(b) with Fig. 6(c) shows that the signal as equalized by the SEA with the skewness scheme retains the low frequency range related to the misalignment, whereas the SEA with the kurtosis scheme ignores this range and highlights the range from 1500 to 4500 Hz. Furthermore, the components at 1500–4500 Hz are filtered out by the SEA with the skewness scheme, but are detected by the SEA with the kurtosis scheme.

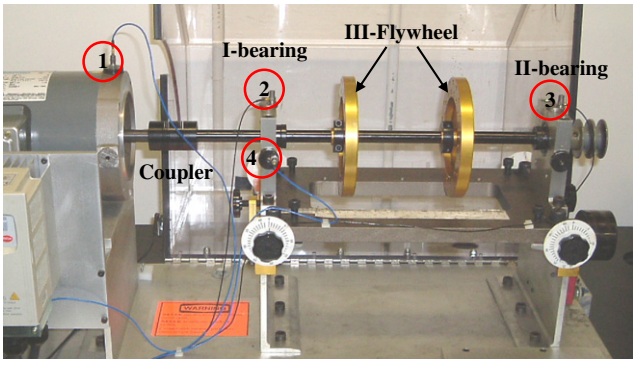

Fig. 5. Simulation test bench and indication of the components.

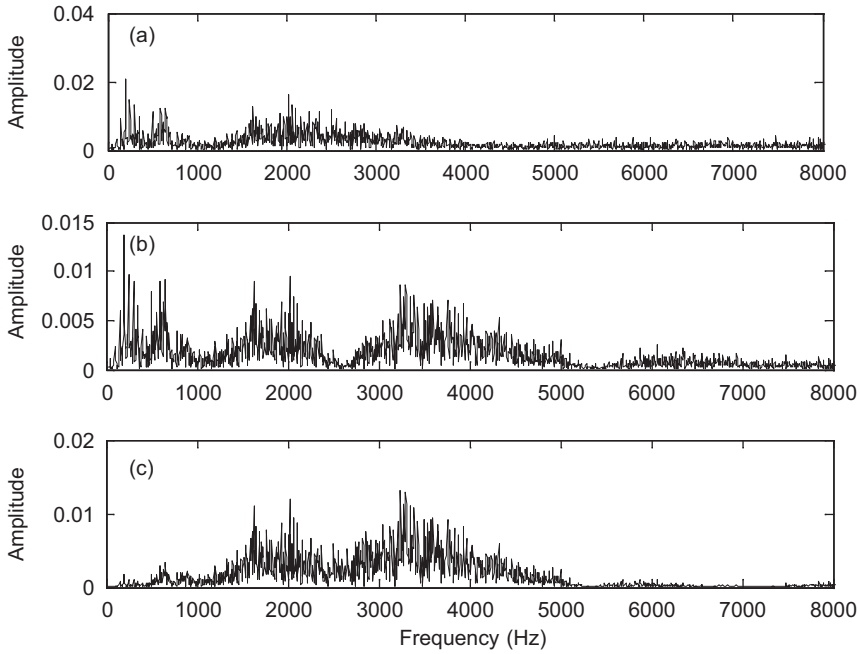

Fig. 6. Spectra of observed and equalized signals of sensor 2 (skewness and kurtosis): (a) spectrum of observed signal of sensor 2; (b) spectrum of equalized signal (third-order); and (c) spectrum of equalized signal (fourth-order).

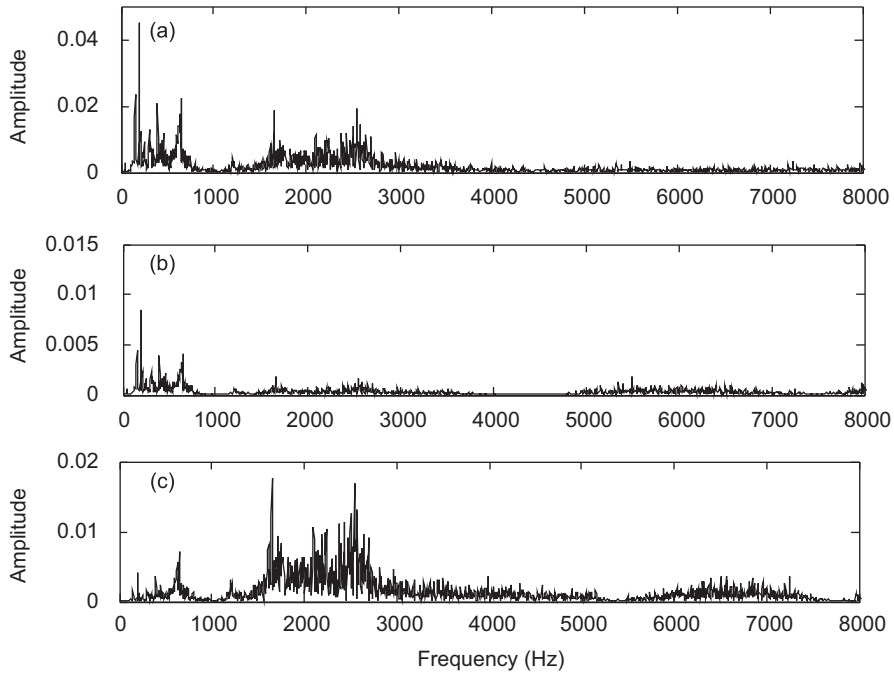

Fig. 7. Spectra of observed and equalized signals of sensor 4 (skewness and kurtosis): (a) spectrum of observed signal of sensor 4; (b) spectrum of equalized signal (third-order); and (c) spectrum of equalized signal (fourth-order).

Correspondingly, the SEA with the skewness/kurtosis schemes and the equalizer length of 16 was applied to the signal from sensor 4. The spectrum of the observed signal of sensor 4 is shown in Fig. 7(a) at the same scale as that in Fig. 6(a). The spectra of the equalized signal after applying the SEA with the skewness and kurtosis

schemes are shown in Figs. 7(b) and (c), respectively. Two components in Fig. 7(a) can be detected. One is related to the misalignment characteristics of the shaft and the resonance of the fundamental frequency (50 Hz), which are located in the low frequency; the other component, which is in the range from 1500 to 3000 Hz, reflects the characteristics of the faulty bearing. In Fig. 7(b), the low frequency range is obviously retained after applying the SEA with the skewness scheme, and much of the energy in the frequency range from 1500 to 3000 Hz is filtered out. However, after applying the SEA with the kurtosis scheme, the spectrum shown in Fig. 7(c) is quite different. The components from 1500 to 3000 Hz are retained and the low frequency components are filtered out.

Hence, from the analysis of sensors 2 and 4 the same conclusion can be obtained: the SEA with the skewness scheme is more suitable for the recovery of a signal with an asymmetric distribution, whereas the SEA with the kurtosis scheme is more efficient in recovering vibration with the abrupt changes, such as the vibration induced by impact.

Bearing vibrations from another test bench were collected to further validate the conclusion. The tested bearing also had a defect in its outer race, and there was a small misalignment of the shaft. Fig. 8(a) shows the waveform and spectrum of the observed signal. The equalized signals and their spectra after the application of the SEA with the skewness and kurtosis schemes are plotted in Figs. 8(b) and (c), respectively. Fig. 8(b)(i) shows a signal with a distinct trend distribution. It is obvious that this equalized signal represents the vibration generated by the shaft as a result of the misalignment. The waveform and spectrum of the equalized signal in Fig. 8(c) show that the impulse is exhibited repetitively within the period of 10 ms in time domain and at a frequency band from 1600 to 3600 Hz in the frequency domain, which are characteristic of bearing vibration generated by a defect in the bearing rolling elements.

4. Analysis of the equalizer length for equalization optimization

In ideal cases, BE works in a model with a single source input and a single output. This model assumes that the observed signal contains only one independent source signal. However, for mechanical vibrations, as shown in Section 3, the observed signal is usually a mixture of independent sources. In addition, the transmission paths from the source points to the measuring points are different because of the different source locations. The equalizer is equivalent to the inverse transform of the process that the source signal is transmitted from the source point to the measured point. The length of the equalizer can reflect the characteristics of the transmission path of the source signal, and thus if we assume that the contributions of the different sources to their mixture are theoretically almost equal, then the effect of equalizer length on BE with the SEA should be considered carefully.

4.1. SEA with different equalizer lengths for a bearing signal

To identify and confirm the problem of equalizer length, the SEA with the kurtosis scheme was applied to the observed signal of sensor 3 described in Section 3.3, but with a different equalizer length. Extensive tests were conducted using different equalizer lengths. The frequency spectrum generated by each length was observed and compared with other spectra generated by other lengths. The two selected equalizer lengths are 14 and 70 for the lower length value and the higher length value, respectively. These two values were used because of the obvious difference in their generated spectra. Fig. 9(a)(i) presents the time waveform of the observed signal. Figs. 9(b)(i) and (c)(i) are the time waveforms of the equalized signals corresponding to the two selected equalizer lengths. The corresponding frequency spectra of these signals are presented in Figs. 9(a)(ii), (b)(ii), and (c)(ii) for the observed signal and the equalized signals of lengths 14 and 70.

The spectra in Figs. 9(a)(ii), (b)(ii), and (c)(ii) show that the characteristic frequency components from 1500 to 3000 Hz are retained. However, the spectrum in Fig. 9(b)(ii) exhibits more high frequency components greater than 6000 Hz, which hold most of the total energy. In addition, it is known that bearing (I) has a defect in the outer race and that bearing (II) is in good condition. Thus, if the equalized signal is generated by bearing (I), then the frequency of the impulse should be the same as the frequency of the BPFO. The BPFO of

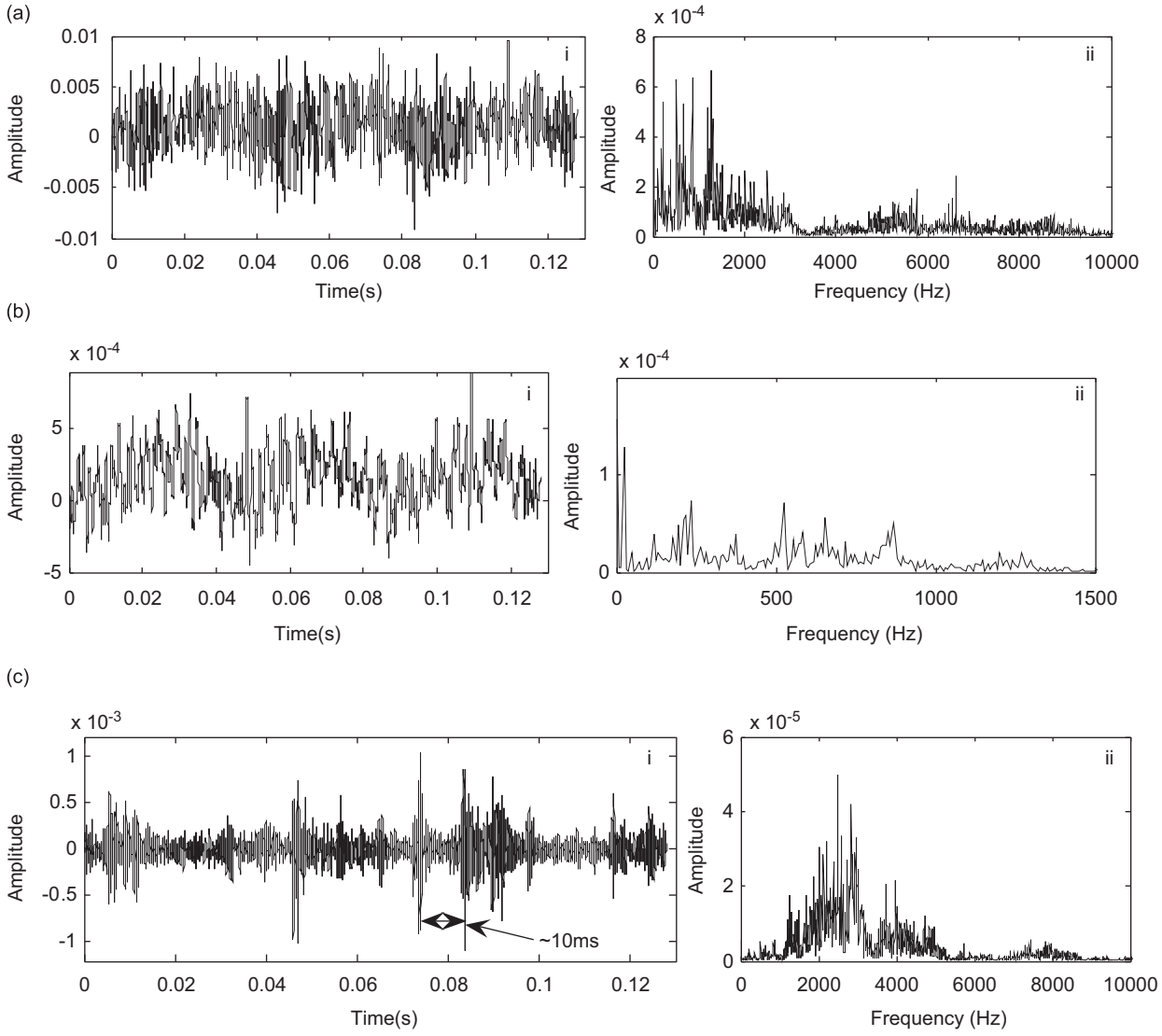

Fig. 8. Observed bearing signal, equalized signals, and their spectra: (a) observed signal and its spectrum; (b) equalized signal and its spectrum (skewness scheme); and (c) equalized signal and its spectrum (kurtosis scheme).

bearing (I) is calculated as

$$f_{\mathrm{od}} = \frac{Z}{2} f_s \left(1 - \frac{d}{D}\cos\,\alpha\right) = 154.5\,\mathrm{Hz}, \tag{14}$$

where the related parameters of the bearing used in the experiments are shown in Fig. 10.

Fig. 9(c)(i) shows that there are 5 impulses at around 32 ms, which is close to the BPFO of 154.5 Hz. This confirms that the equalized signal comes from the vibration generated by bearing (I).

A comparison of the equalized signal spectra when the equalizer lengths of 14 and 70 are applied shows that the bearing vibration frequencies are more prominent and clearer when the equalizer length is 70 than when the length is 14. Hence, to efficiently recover the bearing vibration, an equalizer length of 70 is the more appropriate of the two. For this case, if the equalizer length is over 70, the result will be roughly the same but

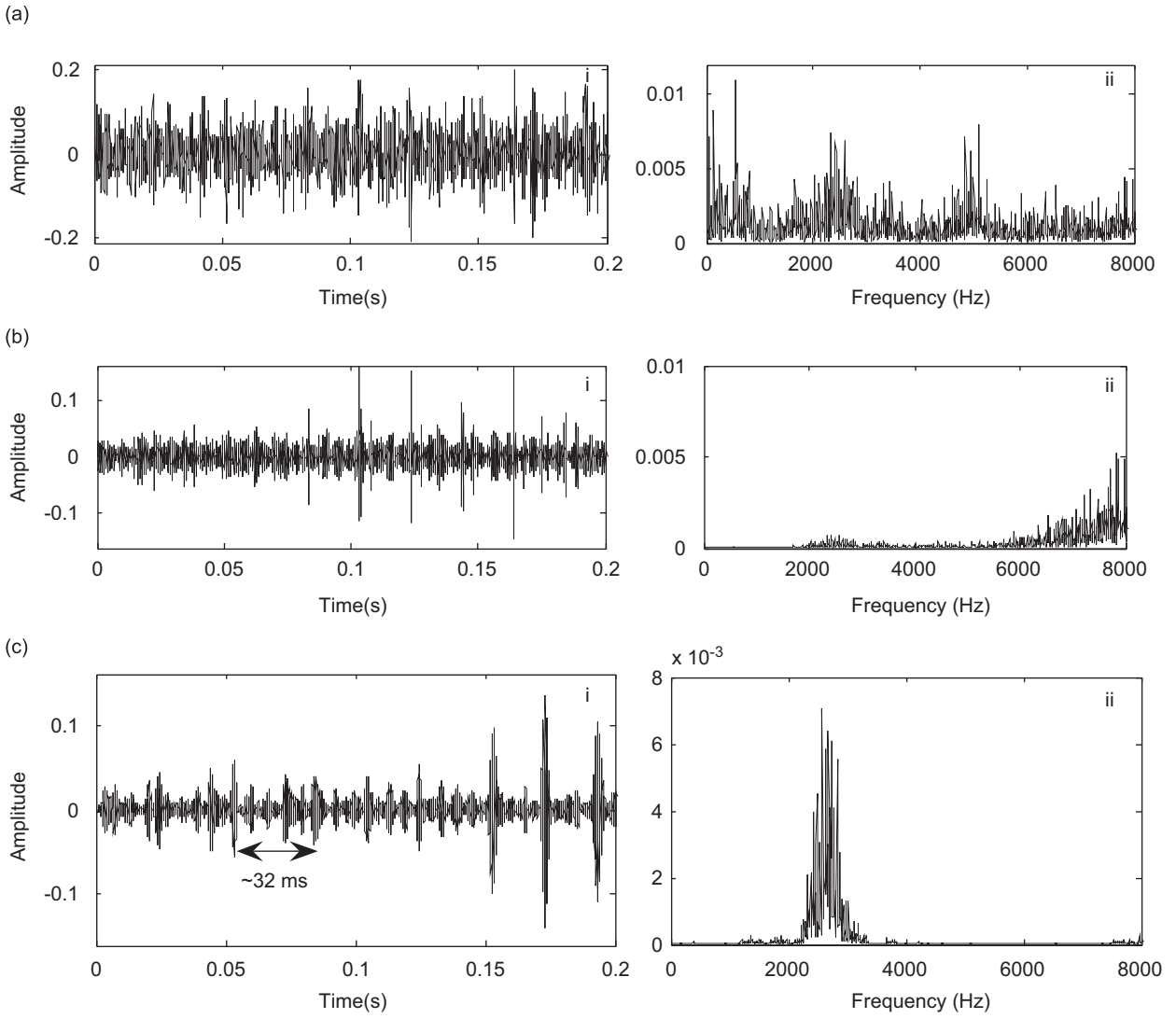

Fig. 9. Observed signal (sensor 3) and equalized signals with different equalizer lengths: (a) observed signal and its spectrum; (b) equalized signal and its spectrum (equalizer length: 14, kurtosis scheme); and (c) equalized signal and its spectrum (equalizer length: 70, kurtosis scheme).

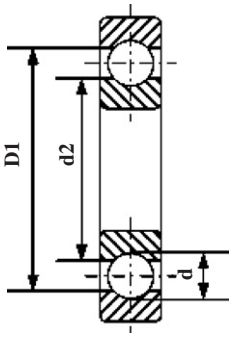

Shaft rotation frequency: $f_s = 50\text{Hz}$
Ball diameter: $d = 7.7mm$
Outer race diameter: $D_1 = 39.4mm$
Inter race diameter: $d_2 = 28.3mm$
Number of rolling elements: $Z = 8$.
Contact angle: $\alpha = 0°$
Pitch diameter: $D = \frac{D_1 + d_2}{2} = 33.8mm$
$\gamma = \frac{d}{D}\cos\ \alpha = \frac{7.7}{33.9}\cos 0 = 0.2275$

Fig. 10. Diagram and parameters of the bearing used in the experiment.

require more computation. Equalizer lengths smaller than 14 may provide effects similar to those gained using equalizer length 14, but too small a value will result in the loss of effect given by the SEA.

4.2. SEA with different equalizer lengths for a motor signal

In the analysis above, both equalized signals obtained after using the SEA with different equalizer lengths can indicate the characteristics of the bearing vibration, the difference being that more high frequency components appear when the equalizer length of 14 is employed. To further demonstrate the effect of the equalizer length on the equalization results, real data from a traction motor used by a subway train were collected for experiments. The tested motor had two faults: a motor eccentric problem due to poor workmanship in the clearance between the rotor and the stator, and an outer-race defect that occurred in the inspected bearing. Maintenance staff confirmed the diagnosis of two faulty components after the motor had been overhauled.

Fig. 11(a) shows the signal collected from the motor, containing the fault-related vibrations generated by both the bearing and the motor. The bearing signal is difficult to identify because it was overwhelmed by the dominant vibration from the faulty motor. The equalized signals after applying the SEA with the kurtosis scheme at equalizer lengths of 16, 44, and 90 are shown in Figs. 11(b)–(d). Obviously, the signal shown in Fig. 11(b) possessed the characteristics of a dominant signal generated by the motor. The period of the waveform is equal to the rotational speed of motor, which is around 40 ms or 25 Hz. The periodic increase and decrease of vibration amplitude was caused by the eccentric problem of the motor. The temporal waveform in Fig. 11(c) shows the existence of quasi-periodic impulses (10 ms per impulsive signal) that are more likely to be caused by the bearing outer-race defect. In Fig. 11(d), which is generated by using a length of 90, the

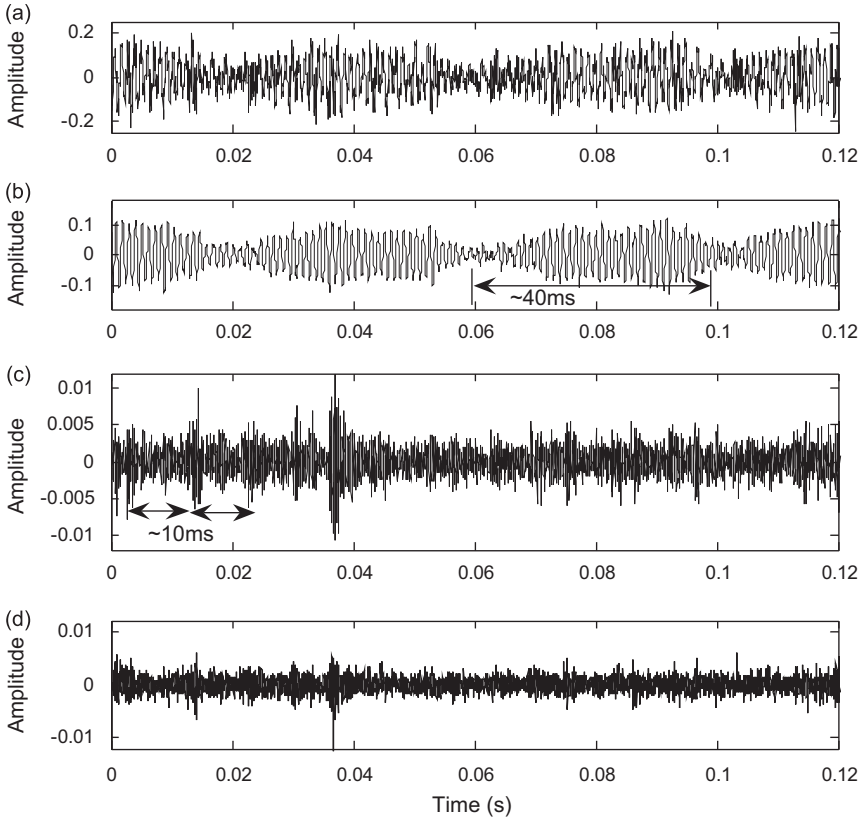

Fig. 11. Observed signal (motor) and equalized signals with different equalizer lengths: (a) observed motor signal; (b) equalized signal (equalizer length: 16); (c) equalized signal (equalizer length: 44); and (d) equalized signal (equalizer length: 90).

quasi-periodic impulses can also be detected, but not as obvious as that shown in Fig. 11(c). Hence, it is confirmed, in some cases, that different source signals can be recovered with the SEA using different optimal equalizer lengths and too high an equalizer length may not benefit the diagnosis of bearing faults.

4.3. Selection of equalizer length

Because equalizer length affects the equalized signals, the correct selection of equalizer length when using the SEA to recover a defect signal should be considered. When the length of the equalizer is approaching or diverging from the length of the inverse filter of the LTI system, the equalized signal is almost the correct estimation of the source signal, and its distribution is almost the same as that of the source signal. In addition, the discussion in Section 3.1 shows that kurtosis and skewness are able to reveal the characteristics of a signal's distribution. The kurtosis and skewness of an equalized signal change little when the length of the equalizer is close to the length of the inverse filter of the LTI system. Hence, when the equalizer length increases, the change in the kurtosis/skewness of the equalized signals shows the degree of match between the equalizer and the inverse filter of the LTI system. If the changes of kurtosis/skewness are great, the equalizer is obviously mismatched with the inverse filter of the LTI system. Based on the above analysis, a method with which to evaluate the degree of matching between the equalizer length and the inverse filter length of the LTI system is proposed.

Assume that $c(i)$, $(i = 1, 2, \ldots, N)$ is the kurtosis/skewness value of equalized signals at different equalizer lengths (i). A performance curve of the rate of change of kurtosis, $c(i)$, versus the equalizer length, i, can be drawn to compare the rate of change of other equalizer lengths. The normalized rate of change, $\mathrm{nc}(i)$, is defined as

$$\mathrm{nc}(i) = \frac{\mathrm{d}c - \min(\mathrm{d}c)}{\max(\mathrm{d}c) - \min(\mathrm{d}c)}, \quad \mathrm{d}c(i) = |c(i+1) - c(i)|. \tag{15}$$

In this kind of performance curve, one can check the zone in which the successive rates of change of kurtosis are relatively small or lower than a suggested threshold. A more appropriate equalizer length can be selected from this zone which has small or low change of rate among a number of successive points. There should be a unique source that can be recovered from this better equalizer length.

Fig. 12(i) shows the curve of the kurtosis value of equalized signal versus the equalizer length for the signal collected by sensor 3 from the test bench as shown in Fig. 5. The performance curve, which is plotted in Fig. 12(ii), shows the relation between the rate of change of kurtosis and the equalizer length. A zone from 42 to 96 (zone 1) can be identified in the figure. The successive rates of change of kurtosis in this zone are relatively small (less than 10%), whereas those below 42 in equalizer length have large successive rates of change. Hence, the equalizer length in zone 1 is considered to be close to the inverse filter length of the LTI

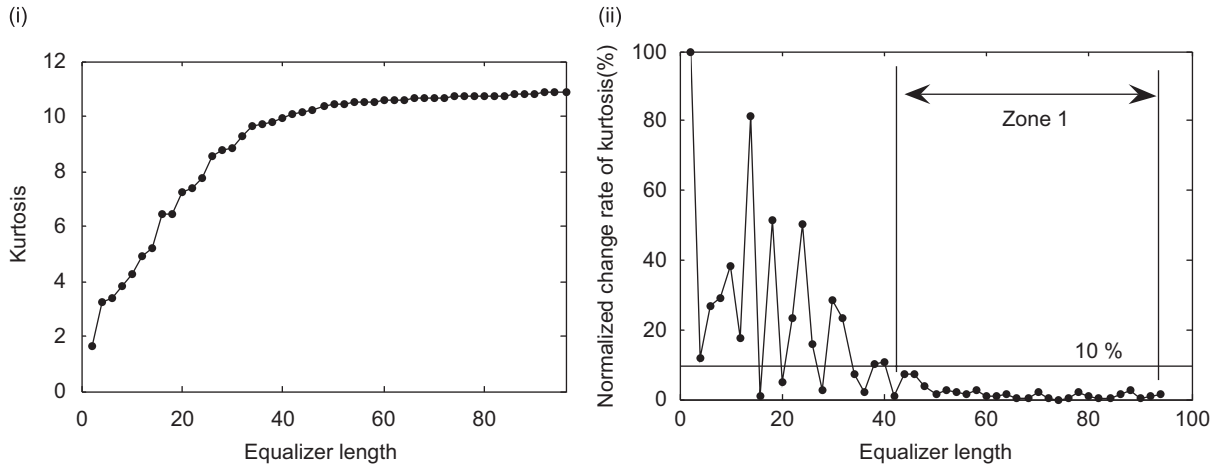

Fig. 12. Performance curve of sensor 3.

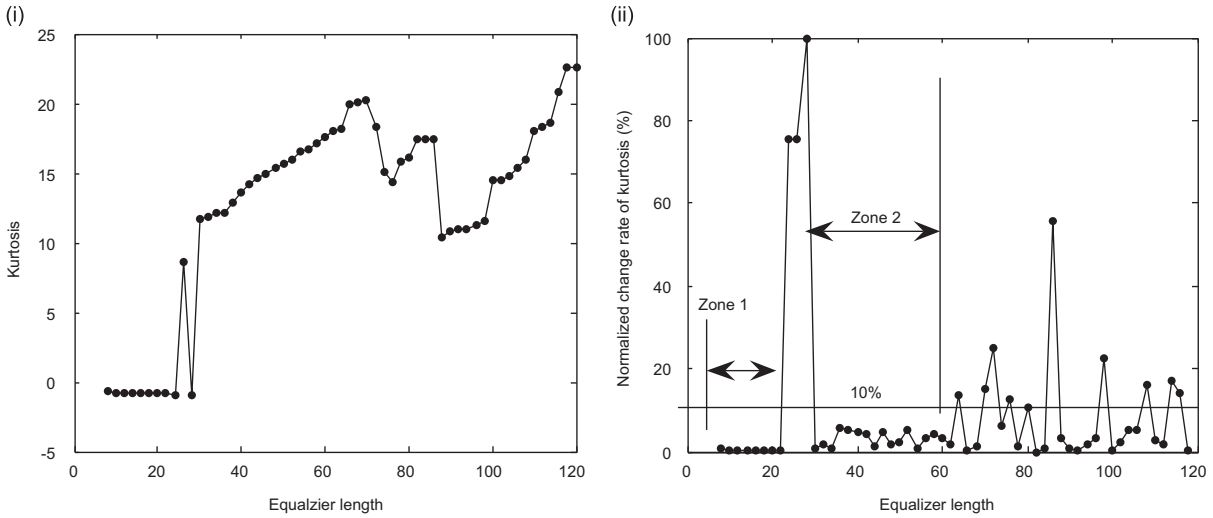

Fig. 13. Performance curve of motor.

system. A better equalized signal can be obtained by applying the SEA with an equalizer length selected from within zone 1, which is verified by the results in Section 4.1. Based on the analysis of the sensor 3 signals in Section 4.1, the value of 10% can be used as a threshold of rate of change to evaluate the performance of equalized signals because at that rate kurtosis becomes small and relatively stable. Hence, the use of other equalizer lengths is not worth trying as the performance cannot be substantially enhanced.

To further verify this method, the signal collected from the subway train's motor as described in Section 4.2 was analyzed. The curve of the kurtosis value of the equalized signal versus the equalizer length and the performance curve are plotted in Figs. 13(i) and (ii). Two zones, which contain relatively small successive rates of change, can be identified from the performance curve. They are the zone 1 (from 6 to 22 in equalizer length) and zone 2 (from 30 to 62 in equalizer length). All of the successive rates of change in kurtosis in zones 1 and 2 are less than the 10% threshold. To make sure that two distinctive source signals can be recovered, one equalizer length should be selected from each of the zones 1 and 2. The selected more appropriate equalizer length from zone 1 is 16 and from zone 2 is 44. The two source signals that are recovered by these two better equalizer lengths are the two vibrations generated by the motor and the bearing (as described in Section 4.2), respectively. Hence, the approach of using performance curve to select a better equalizer length has been verified again.

According to the analysis above, the performance curve is an efficient index with which to reveal the information of the equalized signal, and it provides a good guideline for selecting the optimal equalizer length for the accurate recovery of the source signal. The proposed method of selecting the optimal equalizer length not only reveals the number of source signals contained in the mixed signal, but is also effective in selecting the optimal equalizer length for extracting the source signals from the mixed signal.

5. Conclusion

In this paper, extensive studies of the characteristics of the SEA with kth-order statistic schemes for the analysis of mechanical vibration signals are introduced, and several conclusions are drawn. The SEA with the skewness scheme is more suitable for the recovery of vibration signals with an asymmetric distribution, such as vibration signals that are generated by a misalignment or imbalance, whereas the SEA with the kurtosis scheme is more efficient in equalizing vibrations with abrupt changes in distribution, such as vibrations induced by defects in rolling elements. Hence, the statistic scheme of the appropriate order should be selected according to the distribution or recovery purpose of the signal so that the desired analytical results can be achieved. The effect of the equalizer length on the equalization result is demonstrated and investigated, and it

is shown that different vibrations can be recovered from mixed sources by using the SEA with different equalizer lengths. To achieve the best estimation of a source signal, a performance curve that presents the relation between the kurtosis/skewness of the equalized signal and the equalizer length is introduced to evaluate the equalization result. Based on this performance curve, a method for the selection of the optimal equalizer length is proposed.

The work presented in this paper shows that the SEA is a promising tool for the processing of mechanical vibration signals. However, there are still some problems to overcome in the efficient application of BE to complicated vibration signals, such as the stability of signals in the presence of a high level of background noise, the affiliation identification of source signals, and the recovery of multiple source signals from a single observed signal. Further research would enhance the SEA for more robust and efficient vibration recovery and analysis in the mechanical field.

Acknowledgements

The work described in this paper was fully supported by a grant from the Research Grants Council of the Hong Kong Special Administrative Region, China (Project no. CityU 120605).

References

[1] J.W.A. Fackrell, P.R. White, J.K. Hammond, R.J. Pinnington, The interpretation of the bispectra of vibration signals—II. Experimental results and applications, *Mechanical Systems and Signal Processing* 9 (1995) 267–274.
[2] P. Tse, W.X. Yang, H.Y. Tam, Machine fault diagnosis through an effective exact wavelet analysis, *Journal of Sound and Vibration* 277 (2004) 1005–1024.
[3] P. Tse, Y.H. Peng, R. Yam, Wavelet analysis and envelop detection for rolling element bearing fault diagnosis—their effectiveness and flexibility, *Journal of Vibration and Acoustics—Transactions of the ASME* 123 (2001) 303–310.
[4] Z. Peng, P. Tse, F. Chu, A comparison study of improved Hilbert–Huang transform and wavelet transform: application to fault diagnosis for rolling bearings, *Journal of Mechanical Systems and Signal Processing* 19 (2005) 974–988.
[5] C. Pierre, Independent component analysis: a new concept?, *Signal Processing* 36 (1994) 287–314.
[6] Y. Sato, A method of self-recovering equalization for multilevel amplitude-modulation systems, *IEEE Transactions on Communications* 23 (1975) 679–682.
[7] D. Donoho, *Minimum Entropy Deconvolution, in: Applied Time Series Analysis, Vol. II*, Academic Press, New York, 1981.
[8] Zhinong Li, Yongyong He, Fulei Chu, Application of the blind source separation in machine fault diagnosis: a review and prospect, *Mechanical Systems and Signal Processing* (available online April 27, 2005, in press).
[9] Y. Alexander, L. Amir, P.W. Robert, Blind separation of rotating machine sources: bilinear forms and convolutive mixtures, *Neurocomputing* 49 (2002) 349–368.
[10] G. Gelle, M. Colas, C. Serviere, Blind source separation: a tool for rotating machine monitoring by vibration analysis?, *Journal of Sound and Vibration* 248 (2001) 865–885.
[11] J.Y. Lee, A.K. Nandi, Extraction of impacting signals using blind deconvolution, *Journal of Sound and Vibration* 232 (2000) 945–962.
[12] O. Shalvi, E. Weinstein, Super exponential methods for blind equalization, *IEEE Transactions on Information Theory* 39 (1993) 504–519.
[13] Tongtong Li, J.K. Tugnait, Super-exponential methods for blind detection of asynchronous CDMA signals over multipath channels, *IEEE Transactions on Wireless Communications* 3 (2004) 1379–1385.
[14] Chong-Yung Chi, Chi-Horng Chen, Two-dimensional frequency-domain blind system identification using higher order statistics with application to texture synthesis, *IEEE Transactions on Signal Processing* 49 (2001) 864–877.
[15] Y.F. Wang, P.J. Kootsookos, Modeling of low shaft speed bearing faults for condition monitoring, *Mechanical Systems and Signal Processing* 12 (1998) 415–426.